This document was prepared in conjunction with work accomplished under Contract No. DE-AC09-96SR18500 with the U.S. Department of Energy.

Alternative Materials to Pd Membranes for Hydrogen Purification

Thad M. Adams and Paul S. Korinko
Savannah River National Laboratory, Aiken SC 29803

membrane, hydrogen permeation, alloys

Abstract

Development of advanced hydrogen separation membranes in support of hydrogen production processes such as coal gasification and as front end gas purifiers for fuel cell based system is paramount to the successful implementation of a national hydrogen economy. Current generation metallic hydrogen separation membranes are based on Pd-alloys. Although the technology has proven successful, at issue is the high cost of palladium. Evaluation of non-noble metal based dense metallic separation membranes is currently receiving national and international attention. The focal point of the reported work was to evaluate two different classes of materials for potential replacement of conventional Pd-alloy purification/diffuser membranes. Crystalline V-Ni-Ti and Amorphous Fe- and Co-based metallic glass alloys have been evaluated using both electrochemical and gaseous hydrogen permeation testing techniques..

Introduction

Hydrogen separation and purification has been identified as a bottleneck in the development of advanced hydrogen fuel technologies. Many techniques for hydrogen separation are in use or are currently being investigated, such as cryogenic separation, pressure swing adsorption, catalytic purification and selective diffusion. As a result of its high hydrogen permeability, good mechanical characteristics and highly catalytic surface, which dissociates hydrogen rapidly, palladium is still the membrane material of choice in many applications. Unfortunately, palladium and its alloys are extremely expensive, roughly twice the cost of gold, making them impractical for large-scale applications. Therefore, an economically feasible, palladium-based, commercial scale system would require a significantly reduced amount of palladium, which can be accomplished by techniques such as thin palladium membranes supported on porous substrates or highly permeable bulk substrates. The high cost of palladium has turned the attention of researchers to palladium-free membrane technologies, such as cermets and ceramics for high-pressure, high-temperature applications.

The current generation of gas purification/separation membranes is based on Pd/Pd-alloy used either independently or in conjunction with porous ceramic supports. Palladium/Palladium alloys have been known to possess the ability to dissolve a considerable volume of hydrogen and to demonstrate increasing permeability with increasing pressure differential and temperature. However, the major drawbacks to their industrial use are high cost for Pd, relatively low flux, and that during cycling above and below a critical temperature an irreversible change takes place in the palladium lattice structure which can result in significant damage to the membrane. Palladium coated ceramic membranes offer the potential for extended temperature range operations but suffer from the fatal flaw of "pinhole" short circuit paths. Any "pinholes" in the Pd-catalytic film on the surface of the ceramic substrate will allow for contaminant/intermediate species to pass directly through the membrane thus effectively reducing the purification factor of the membrane. Recent efforts in the hydrogen purification/separation membrane community have focused on the development and evaluation of non-palladium based membranes that offer a lower cost, high flux, and highly durable membranes to replace Pd-based systems. Group 5A metals such as V, Nb, and Ta are currently being evaluated by numerous researchers and show promising results with respect to hydrogen permeability[1-3]. However, these metals suffer from severe hydrogen embrittlement and thus are unacceptable for membranes. Japanese researchers have begun to evaluate alloying additions—Al, Ni, Co, and Mo—to vanadium in hopes decreasing the susceptibility to hydrogen embrittlement [4-5}.

Crystalline Non-Noble Metal Membranes

The most interesting recent result has been the evaluation of Ni-Ti-Nb alloys for hydrogen permeation [6]. Ni-Ti has long been known as a shape memory alloy but it also possesses good hydrogen solubility and mechanical properties. The major drawback is that hydrogen diffusivity in Ni-Ti is considerably slower than either Pd/Pd-alloy, V, Nb, or Ta. In attempt to enhance the diffusivity, additions of Nb have been made to Ni-Ti alloys and permeation and mechanical stability have been evaluated. The limited study of a these ternary Nb-Ti-Ni alloy has shown permeation on an order equal to pure Pd and reasonable mechanical stability in hydrogen. Recent work on V-Ti-Ni and Ta-Ti-Ni alloys by the same authors has shown similar results. The permeabilites of the V- and Ta-alloys were not quite as high as either Pd or the previous studied Nb-alloys [7]. This was attributed to the inherent greater permeability of bulk Nb in comparison to V and Ta.

Amorphous Non-Noble Metal Membranes

The development of metallic glasses in bulk form has led to a resurgence of interest into the potential utilization of these materials for a variety of applications. Prior to this development, metallic glasses were produced exclusively in very thin sections by rapid solidification processing in most cases. The subsequent consolidation into something "bulk" frequently led to devitrification and a loss in the desirable properties characteristic of the glass. In fact, the unique properties of metallic glasses — strengths of 1-2 GPa, toughnesses of 30-70 MPa $m^{-0.5}$, good environmental resistance and unique magnetic properties in some cases — have only been exploited in a few applications where thin sections are desirable (e.g., transformer sheet and magnetic strips for anti-theft tags). A potentially exciting application for these new bulk metallic glass materials is use as membranes for enhancing the efficiency of gas separations both in production processes and for fuel cell usage.

The current generation of gas separation membranes is based on Pd/Pd-alloy used either independently or in conjunction with porous ceramic supports. Palladium/Palladium alloys have been known to possess the ability to dissolve a considerable volume of hydrogen and to demonstrate increasing permeability with increasing pressure differential and temperature. However, the major drawbacks to their industrial use are the high cost for Pd/Pt, relatively low flux, and an irreversible structural change that occurs when the materials are cycled through a critical temperature range. This irreversible change takes place in the palladium lattice structure and can result in significant damage to the membrane. SRNL has previously worked with thin section (melt–spun ribbons) of metallic glass materials for membrane applications, however, with the relatively new ability to cast fully amorphous metallic glasses in bulk sections a new opportunity is opened for bulk metallic glasses as hydrogen membranes. The ability to readily cast metallic glass alloys will allow for easier fabrication of membranes—machine thin membranes from larger castings-- and will also ease mass production challenges in comparison to thin section (melt spun) metallic glass ribbons. Bulk metallic glass alloys are traditionally processed from multi-component system comprised of metallic species of varying atomic size. It is this vast difference in atomic sizes that results in slow diffusion/redistribution kinetics and allows for deep undercoolings to the point of freezing in the "liquid" structure to produce amorphous metallic alloys at relatively slow cooling rates (10-100 K/s). These metallic glass alloys have been shown to possess high permeation rates. For example the permeation rate for a --Zr-Al-Co-Ni-Cu BMG alloy --1.13 x 10^{-8} mol/m s $Pa^{½}$--is comparable to permeation the rate measured for pure Pd metal. Furthermore, these metallic glass alloys have also been shown to possess high elastic toughness and excellent resistance to hydrogen degradation, i.e., structural changes. Both of these properties—high permeation and high elastic toughness--potentially make these materials attractive for gas separation membranes.

The focal point of this work is to extend the Nb-Ti-Ni membrane development work with a direct replacement of Nb with V. Characterization of the resulting microstructure and measurement of the permeability of the novel V-based alloy is reported.

Experimental Approach

Electrochemical Permeation Testing

Arc melted buttons of approximately 25 gms each were prepared using a Centorr System VII arc melter system with a tungsten electrode. Arc melting was performed following evacuation to approximately 10^{-4}Torr and backfilled with argon. The V-Ti-Ni alloys were prepared using 99.7%V, 99.95%Ti, and 99.95% Ni raw materials supplied by Alfa-Aesar. The V-Ni-Ti alloy tested as part of this study contained the following alloy composition—53wt%V, 26wt%Ti, and 21wt%Ni. Characterization of the as-cast microstructure was performed using light optical microscopy on polished and etched samples. Scanning electron microscopy and energy dispersive x-ray spectroscopy—including X-ray dot mapping—using a Hitachi S3600 were performed to characterize the phase structure and a alloying element distribution. Disk approximately 12mm in diameter and 0.5-0.75mm in thickness were sectioned from the arc melted buttons and prepared via grinding on SiC papers to provide a 1200 grit finish.

Hydrogen permeation testing was conducted using a Devanathan and Stachurski type-electrochemical apparatus—Figure 1. Permeation testing of V-Ni-Ti alloy was conducted on foils approximately 0.6mm in thickness with an exposed surface area of 0.4 cm^2. The test solution consisted of 0.1M NaOH solution at room temperature. The solution was purged with nitrogen 24 hours prior testing as well as during the test. The electrochemical parameters included a charging current of 100μA/cm^2 on the cathode side and an applied potential of -125mV versus a saturated calomel electrode on the anode side. In an attempt to truly measure the actual permeability of the V-Ni-Ti alloy both sides of the alloy disc were coated with a flash layer of Pd. As a means of comparison Pd foils approximately 0.25 and 0.5mm in thickness have been tested under identical conditions.

Figure 1. Devanathan-Stachurski Electrochemical Hydrogen Permeation Apparatus

Analysis of the electrochemical data provides a measure of the hydrogen flux through the sample by measuring the steady-state current density I_p (A/cm^2) on the anodic side of the cell. This steady state current density can be converted to the steady state hydrogen permeation flux, J_∞, (mol/m^2s) via equation 1 below.

$$J_\infty = I_p/nF \quad (1)$$

The steady-state hydrogen permeation rate, V, (mol/m s), can be defined according to equation 2

$$V = J_\infty L = LI_p/nF \quad (2)$$

where L is the sample thickness, I_p is the steady-state current density, n is the number of electrons transferred, and F is Faraday's constant.

Gas Permeation Testing

Hydrogen permeation testing was conducted using the permeation test rig shown in Figure 2. Samples, 19 mm diameter and 0.89 mm thick or disks were welded into 2.12" diameter Conflat (CF) flanges. Crevices were seal welded using electron beam welding

to minimize the effects of virtual leaks. The sample assemblies were placed in a 1" OD vacuum system fabricated with 2.12" CF flanges. Copper gaskets were used to seal the samples. The samples were evacuated to at least 1 x 10-6 Torr for a period of at least four hours at room temperature. The samples were then heated to 100C for 8 to 16 hours to outgas the system and up to the final test temperature. A leak rate test was conducted by closing the appropriate valve. If the leak rate was not linear, the sample was evacuated for additional time, after an acceptable leak rate curve was obtained, the sample section valves were closed and the desired pressure of deuterium was introduced. It took approximately 2-3 minutes for the pressure to reach the target value. The pressure rise on the low pressure side of the system was monitored. The data were logged at either a ten to 30 second interval. The data were reduced to estimate the diffusivity and permeability.

Figure 2. SRNL Gaseous Permeation Test Rig

The raw data were plotted as a function of time. The data exhibit three distinct regions, the background in-leakage region, a transition region, and a steady state region, nearly linear region. The diffusivity (D) was estimated by calculating the slope and the intercept of the linear region using a least squares method. These two variables were then used to determine the lag time (tl), i.e., the time at which the line crossed the y-axis at zero. Lag time, tl, time was used in the equation: tl = x2 / 6 D (1) to determine D. The permeability (Φ) was estimated from the slope (M) of the curve, the expansion volume (V), the sample area (A), and the test pressure (ΔP) as shown in Eq. 2. $\Phi = M * V * t / A \sqrt{\Delta P}$ (2). The permeability is the product of the solubility (S) and the diffusivity as shown in Eq. 3. $\Phi = S * D$ (3)

Results and Discussion

Microstructure Analysis

Evaluation of the microstructure of the V-Ti-Ni alloy was performed using scanning electron microscopy combined with x-ray mapping of the element constituents. Previous work on Nb-Ti-Ni alloys being investigated for advanced hydrogen separation membrane use has attributed positive results to microstructures consisting of a large primary $Nb_{83}Ti_{13}Ni_4$ phase surrounded by eutectic (NiTi +NbTiNi); $Nb_{83}Ti_{13}Ni_4$ was postulated to be the high diffusivity phase while the eutectic structure contributes to the lack of susceptibility to hydrogen embrittlement [6]. SEM backscattered and secondary electron micrographs of the V-Ti-Ni alloy display a similar microstructure to the Nb-Ti-Ni alloy with a primary phase surrounded by interdendritic eutectic structure—Figure 2. X-ray mapping of the elemental constituents provided in Figure 3 shows the primary phase in the microstructure to be high in vanadium content. Additionally, the interdendritic eutectic is rich in Ni and Ti. Semi-quantitative chemical analysis of the composition of the vanadium rich primary phase indicates an approximate composition of $V_{75}Ti_{16}Ni_9$.

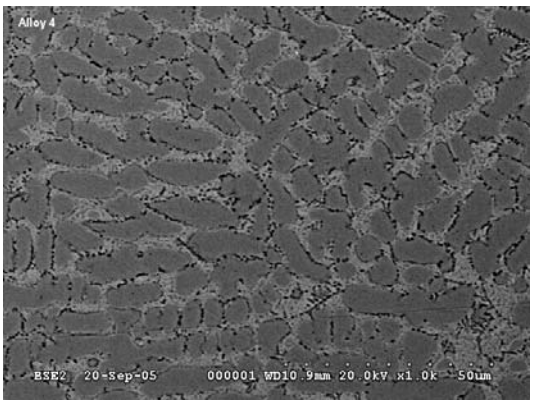

(a)

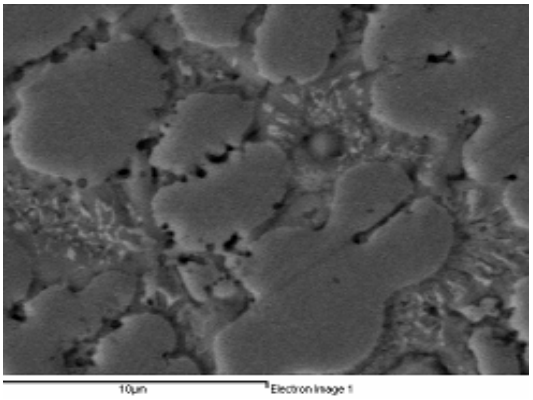

(b)

Figure 2. Scanning Electron Microscope Images of a V53-Ti26-Ni21 Alloy (a) Back-scattered and (b) secondary electron image.

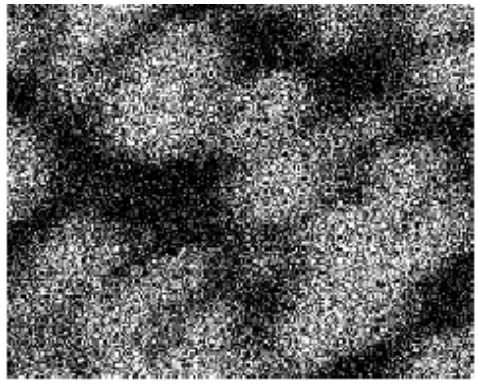

V Ka1

(a)

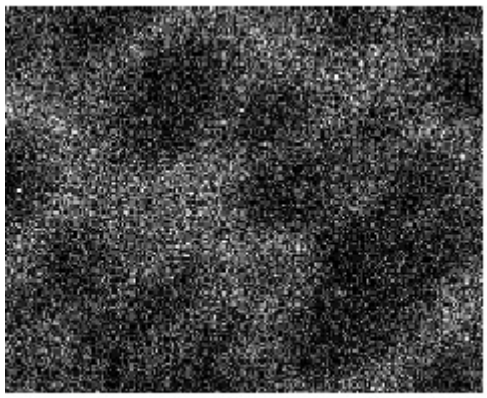

Ti Ka1

(b)

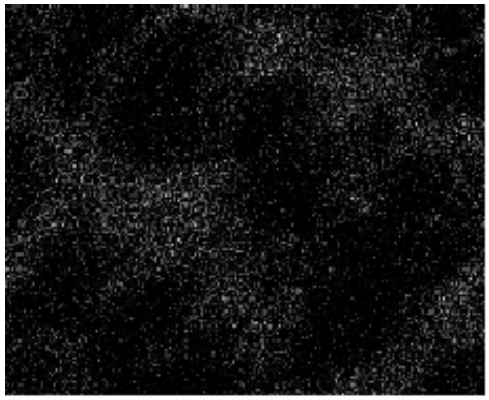

Ni Ka1

(c)

Figure 3. X-ray Mapping of Elemental Constituents within the micrsotructure of a V53-Ti26-Ni21 membrane alloy: (a) V-Kα1 map, (b)Ti Kα1 map, and (c) Ni-Kα1 map.

Electrochemical Hydrogen Permeation

Measurement of the steady state hydrogen permeation flux and rate was conducted and compared to measured values for pure palladium. Comparison of the results for the V-Ti-Ni all to palladium since Pd/Pd-alloys are the current dense metallic membrane materials of choice. The testing was conducted under similar condition—100μA/cm^2 charging current at 22°C-- using the apparatus previously shown in Figure 1. A single set of results are shown in Figure 4, graphed as current density versus time. Examination of the current density plots for the two alloys shows an almost order of magnitude higher steady state current density value for the Pd membrane when compared to the V-Ti-Ni alloy. This higher steady state current density translates into a larger steady state hydrogen flux through the Pd membrane. However, due to the significant difference in thickness between the two membrane materials—L_{Pd}=0.05mm and L_{V51}=0.635mm—the overall hydrogen permeation rate as calculated from equation 2 is larger by an order of magnitude for the V-Ti-Ni alloy. Table 1 displays the calculated steady-state permeation rates for both materials. Thus, from these initial low temperature results the V-Ti-Ni alloy appears to possess a hydrogen permeability greater than Pd under the same conditions. Finally, additional testing at higher cathodic charging currents showed increasing anodic current densities that appeared to saturate .

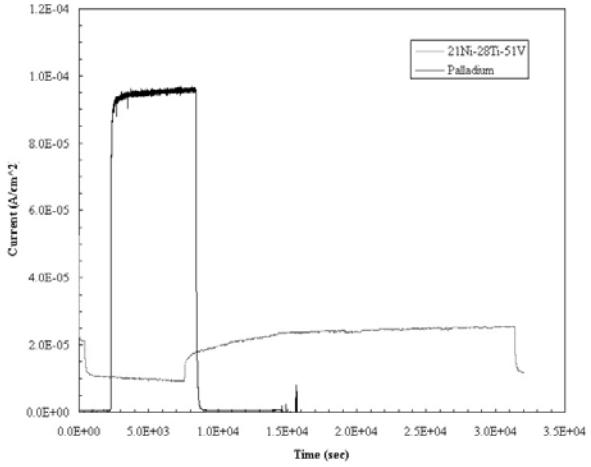

Figure 4. Measured Anodic Current Density During Electrochemical Hydrogen Permeation Testing for Pd and V-53-Ti26-Ni21 materials at 22°C.

Table 1. Steady-State Hydrogen Permeation Rates Measured for Pd and V-Ti-Ni Alloy

Alloy	Permeation Rate (mol H_2/m s)
Palladium	**3.3-4.3 x 10^{-10}**
V53-Ti26-Ni21	**1.0-3.7 x 10^{-9}**

Gaseous Hydrogen Permeation Testing

Measurement of the steady state permeation flux for both the crystalline V-Ti-Ni alloys (see microstructure of V51-Ti28-Ni21 and V54-Ti28-Ni18 alloys in Figure 5) and the amorphous metallic glass materials was conducted and compared to literature data for palladium membranes. The testing was conducted under sub-atmospheric pressures but at values typically used at the Savannah River Site for hydrogen isotope purification. A typical raw data curve for a V51-Ti28-Ni21 alloy at a temperature of 400°C and a pressure of 10 torr is shown in Figure 6. The

calculated permeabilities from test data collected at 400°C for this alloy as well as for a V54-Ti28-Ni18 alloy are provided in Table 2.

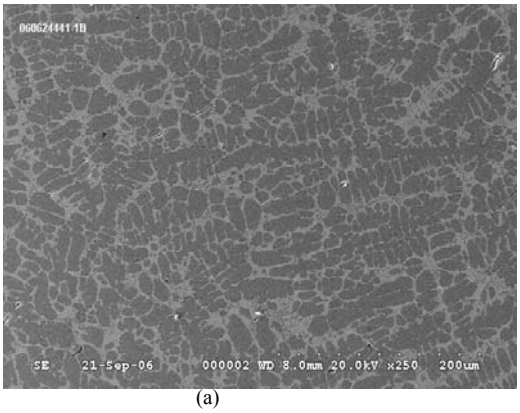

(a)

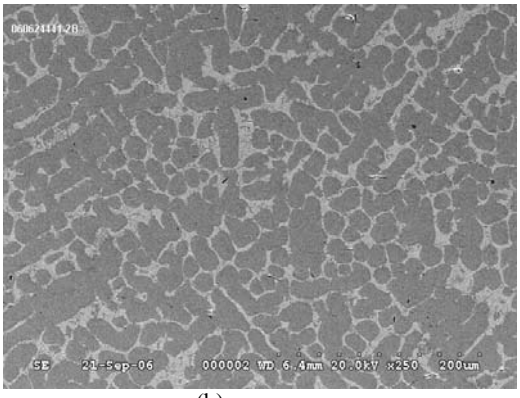

(b)

Figure 5—SEM-backscattered electron images of the microstructures of (a) V51-Ti28-Ni21 and (b) V54-Ti28-Ni18 alloys

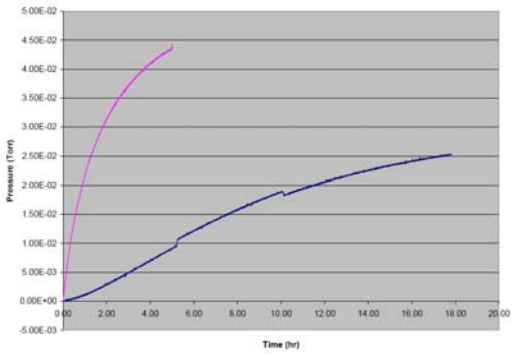

Figure 6. Hydrogen saturation test data for V51-Ti28-Ni21 Alloy.

Table 2—Permeability Values for V-Ti-Ni alloys Tested at 400°C

Alloy	Permeability (mol H_2 m^{-1} s^{-1} $Pa^{-1/2}$)
V51-Ti28-Ni21	1.26×10^{-8}
V54-Ti28-Ni18	9.71×10^{-9}

Similar to Pd and Pd-alloy membrane materials the V51-Ti28-Ni21 alloy demonstrated a susceptibility to hydriding when cooled through a critical temperature range in the presence of hydrogen. During testing a system power failure allowed the sample to cool from the test temperature (400°C) to room temperature under hydrogen. During re-start of the system it was determined that the sample has failed and this failed sample was then examined using x-ray diffraction in order to determine the cause of failure. Results from the XRD analysis shown in Figure 7, clearly show the formation of vanadium- hydride phase in this sample which resulted in the subsequent failure of the membrane.

In addition to the V-based alloys, metallic glass materials have been tested using the same approach, temperature range and pressures. Due to concerns about crystallization of the material, the samples were fixtured in 0.75" diameter VCR fittings using silver plated nickel gaskets. The samples were verified leak tight to at least $2x10^{-9}$ sccm He. The commercial-off-the-shelf (COTS) metallic glass material tested exhibits a permeability and flux within two decades of Pd. The raw data are shown in Figure 8. Due to the low thickness of this sample, approximately 25μm, no determination of a lag time was possible. Testing using a mass spectrometer generally indicated hydrogen at near saturation levels within the first sampling frequency, which is limited to about 15 seconds for the instrumentation used. The data were analyzed using the standard data reduction method and the permeability of this alloy is indicated in Table 3.

With the relative promise of this material and its relatively high strength, testing of additional COTS materials is on-going and will be reported in future articles.

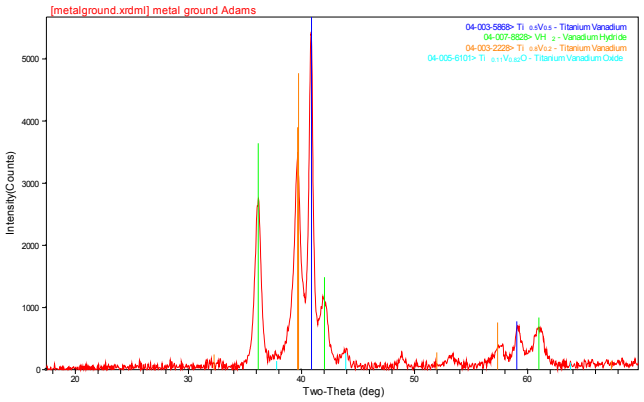

Figure 7. XRD data indicating formation of vanadium hydride on cooling to room temperature under H_2 cover gas.

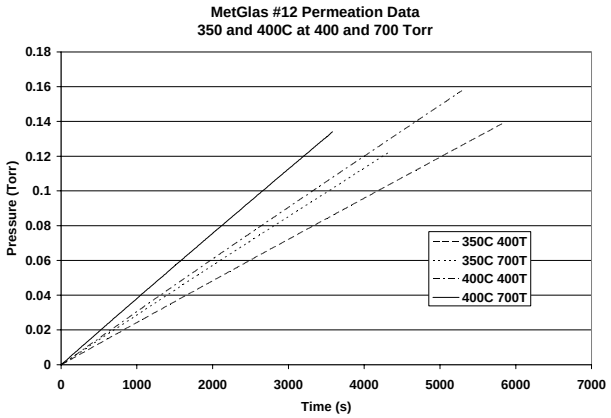

Figure 8. Permeation data for a typical MetGlas sample

Table 3—Permeability data for COTS metallic Glass materials compared to Pd

Alloy	Permeability (mol H_2 m^{-1} s^{-1} $Pa^{-1/2}$)
Palladium 350°C	**1.8×10^{-8}**
Palladium 400°C	**2×10^{-8}**
MetGlas 12 350°C	**1.81×10^{-9}**
MetGlas 12 400°C	**1.94×10^{-9}**

Conclusions

V-Ti-Ni alloys and Fe- /Co-Based metallic glasses have been evaluated with respect to hydrogen permeability for potential use in hydrogen purification membrane reactor application. Microstructural characterization of the V-Ti-Ni alloy using SEM has shown similar microstructural features to a previously evaluated Nb-Ti-Ni alloy; namely, the occurrence of a primary phase surrounded by interdendritic eutectic..

Hydrogen permeation rate for a V53-Ti26-Ni21 alloy was measured electrochemically and compares favorable to rates also measured for pure Pd. Subsequent, gaseous hydrogen permeation testing of similar V-Ti-Ni alloys once again demonstrated permeabilites on par with commercially available Pd/Pd-alloy membrane materials. Permeation testing of the Fe-/Co-based metallic glass alloys demonstrated permeabilities slightly lower than Pd/Pd-alloys however, the cost savings afforded by these materials (approximately 650X lower) warrants further study/evaluation of this class of materials.

Reference

1. R. E. Buxbaum and T. L. Marker, Journal of Membrane Science, 85, 29-38, (1993).
2. N. M. Peachey, R. C. Snow, and R. C. Dye, Journal of Membrane Science, 111, 123-133, (1996).
3. T. S. Moss,N. M. Peachey, R. C. Snow, and R. C. Dye, International Journal of Hydrogen Energy, 23, 99-106, (1998)
4. C. Nishimura, M. Komaki, S. Hwang, and M, Amano, Journal of Alloys and Compounds, 330-332, 902-906, (2002).
5. Y. Zhang, T. Ozaki, M. Komaki, and C. Nishimura, Scripta Materialia, 47, 601-606, (2002).
6. K. Hashi, K. Ishikawa, T. Matsuda, and K. Aoki, Journal of Alloys and Compounds, 368, 215-220, (2004).
7. K. Hashi, K. Ishikawa, T. Matsuda, and K. Aoki, Journal of Alloys and Compounds, 404-406, 273-278, (2005).